Scaling of heat transfer and temperature distribution in granular flows in rotating drums

B. Yohannes,[1] H. Emady,[2] K. Anderson,[3] I. Paredes,[3] M. Javed,[3] W. Borghard,[3] F. J. Muzzio,[3]
B. J. Glasser,[3] and A. M. Cuitiño[1,*]

[1]*Mechanical and Aerospace Engineering, Rutgers University, Piscataway, New Jersey 08854, USA*
[2]*Chemical Engineering, Arizona State University, Tempe, Arizona 85287, USA*
[3]*Chemical and Biochemical Engineering, Rutgers University, Piscataway, New Jersey 08854, USA*

(Received 15 January 2016; published 14 October 2016)

Accurate prediction of the time required to heat up granular materials to a target temperature is crucial for several processes. However, we do not have quantitative models to predict the average temperature or the temperature distribution of the particles. Here, we computationally investigate the scaling of heat transfer in granular flows in rotating drums. Based on our simulations, which include a wide range of system and material properties, we identify the appropriate characteristic time that is used to derive equations that predict the particles' average temperature and the particles' temperature distribution.

DOI: 10.1103/PhysRevE.94.042902

I. INTRODUCTION

Many industrial processes, such as calcination, powder metallurgy, and the production of ceramics, involve thermal treatment of granular materials and powders [1], and rotating drums (kilns) are one of the more popular devices used for these processes [2]. The thermal treatment of granular materials and powders in rotating kilns is extremely energy intensive, and, for example, the thermal treatment of powders during cement production alone is estimated to utilize 1% to 3% of the world's total energy consumption [3]. The main purpose of the thermal treatment is to raise the temperature of the material to a target temperature so that a desired chemical or physical process takes place. To predict the time it takes to reach the target temperature is essential for a high quality product and for economical operation. If the target temperature is not reached or if the particles are not kept at the target temperature for an adequate time, the intended process (or conversion) will not occur. It is also essential that all particles are heated up to the target temperature as the particles which remain below the target temperature will not be processed, which could significantly affect the uniformity of the final product.

Numerous experimental [2,4–9], theoretical [10], and computational [3,11,12] studies have been done on heat transfer, flow regimes, and mixing in rotating drums. The presence of various heat transfer mechanisms and the intensive mixing, accompanied by the interaction of particles, make the study of heat transfer in rotary drums challenging and difficult to predict [6,11,13]. In general, the heat transfer mechanisms include conduction through the solid, conduction through the contact area between particles, conduction through the interstitial gas film between particle-particle and wall particle contact [5,14], convection by the fluid, and radiation between the surfaces of particles and the drum. At low temperatures (less than about 700 K) and in the absence of highly conductive flowing fluid, which results in low Biot number ($\mathrm{Bi} = \frac{hd}{k} < 1$), where h is the heat transfer coefficient of the gas, d is the size of the particles, and k is thermal conductivity of the particles, the rate of heat transfer is dictated mostly by the thermal conduction through particle contacts [10,11]. For such systems, using a lumped parameter formulation, the rate of change of the average temperature $\bar{T}$ can be represented as $MC_p\frac{d\bar{T}}{dt} = \alpha A_s(T_w - \bar{T})$; M and C_p are the total mass and specific heat capacity of the granular material, respectively; α and A_s are the heat transfer coefficient and contact area at the interface of the granular material and rotating drum, respectively; and T_w is the temperature of the drum wall [12]. $\bar{T}$ at time t can be computed from the analytic solution of the lumped parameter formulation as

$$\frac{T_w - \bar{T}(t)}{T_w - T_o} = e^{-\frac{t}{\tau}}, \tag{1}$$

where T_o is the initial temperature of the particles. The only parameter that is required to compute $\bar{T}$ is the rate parameter $\tau = \frac{MC_p}{\alpha A_s}$, referred to as the *thermal time* of the granular system. τ is the time at which $T_w - \bar{T}$ drops by about 63%.

However, how τ scales with the system size and material properties is not well understood. There are several models that have been developed based on experiments and penetration theory [1,2,4,10]. Most of these models are based on bulk material properties, such as bulk density and bulk thermal conductivity, rather than particle properties. Some prior studies have attempted to estimate scaling of heat transfer and heat transfer mechanisms using particle scale dimensionless parameters. For example, Figueroa *et al.* [11] used the Péclet (Pe) and the Nusselt numbers to define scaling of heat transfer in a rotating drum via discrete element method (DEM) simulations. The relationship between these dimensionless numbers was found to be the same for a given geometry and material type, but the relationship didn't possess universality across various material properties and scales. They suggested that a better model should include properties of agitated granular materials as well as the microstructure, and showed that at low Pe the heat transfer is dominated by interparticle conduction, whereas at high Pe the convection and mixing of hot particles are the dominant mechanisms of heat transfer. Similarly, Rognon and Einav [15] showed that the heat flux density is a function of a thermal number, a dimensionless parameter defined as the ratio of the inertial time (timescale for rearrangement of particles'

*cuitino@jove.rutgers.edu

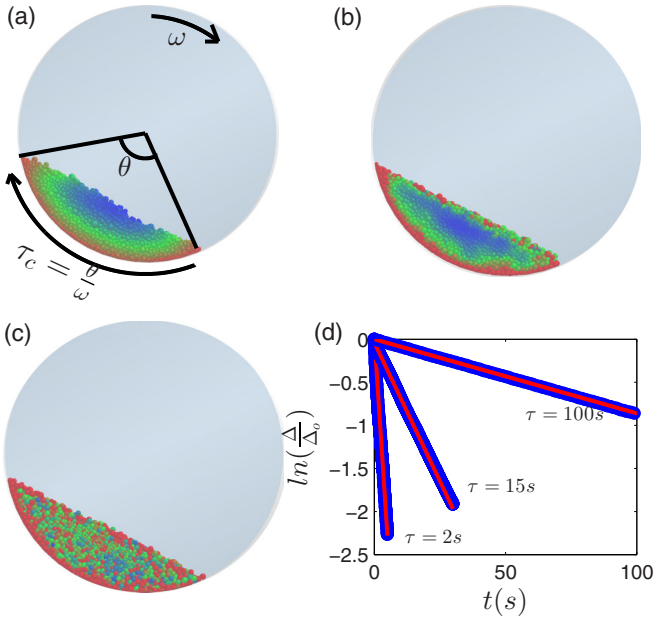

FIG. 1. Snapshots from a rotating drum simulation: (a) $\phi = 0.05$, low ϕ case—particles heat up like a solid body, (b) $\phi = 1.2$, intermediate ϕ case—particles heat up with a cool inner core, and (c) $\phi = 35$, high ϕ case—particles heat up relatively uniformly. Particles are colored based on their temperature (red $= T_w$ and blue $= T_o$). ω is the speed of rotation, θ is the fill angle, and $\tau_c = \frac{\theta}{\omega}$ is the time a particle spends in contact with the drum wall. (d) Computation of the thermal time parameter τ from DEM simulations. $\Delta = T_w - \bar{T}$, and $\Delta_o = T_w - T_o$. The results from the DEM simulations (•) are consistent with the lumped parameter formulation (−) [Eq. (1)].

position) [16] and timescale related to the rate of particles' temperature change in simple sheared granular flows. The heat flux density due to contact conduction is constant for a given material, while the heat flux due to granular convection, caused by velocity fluctuations, increases with the thermal number. In rotating drums, the granular convection heat flux is directly related not only to the velocity fluctuations, but also to the mixing of the particles due to the drum rotation. Emady *et al.* [3] identified another dimensionless time parameter ϕ, which is the ratio of the thermal time of a single particle, τ_p Eq. (2), to the average contact time between a particle and the heated, rotating drum wall, τ_c [Fig. 1(a)]. It was found $\frac{\tau}{\tau_c}$ increases proportionally to ϕ, and the relationship holds for different values of thermal diffusivity. In addition, they showed that a uniform particle temperature is achieved at higher values of ϕ, whereas a wider temperature distribution is achieved at lower values of ϕ.

For a better appreciation of these dimensionless time parameters and to get a better picture of the inherent heterogeneity in granular materials, understanding the relationship between these parameters, and their role in defining a scaling law for heat transfer and temperature distribution is crucial. In this article, we present a quantitative scaling relationship for heat transfer that can be used to predict τ and track the distribution of particles' temperature in rotating drums based on DEM simulations. We show that the scaling relationship is valid for various mechanical, physical, and thermal properties of the particles and a wide range of flow conditions.

II. THEORY AND SIMULATION SETUP

Hertz and Mindlin contact theories are used in the simulations to compute the particle-particle and particle-wall contact forces [17]. The heat transfer between particles is only through the contact area between the particles. The heat flux between two particles is $Q_{ij} = H_c(T_j - T_i)$, where H_c is the thermal conductance given as the product of the thermal conductivity k and the contact radius a 11,12,18,19]. From Hertz's contact theory for spherical particles, it is possible to show that $a = (\frac{3Pd}{2E^*})^{\frac{1}{3}}$, where P is the contact force between particles and E^* is the elastic stiffness of the particle. For nonspherical and rough particles there is no unique relationship between a and d. The relationship will change as the orientation of the particles change. For spherical particles the rate of temperature increase for each particle is then computed as $\frac{dT_i}{dt} = \frac{Q_i}{\rho_i C_{pi} V_i}$, where Q_i is the summation of all Q_{ij} involving particle i, and ρ_i, C_{pi}, and V_i are the mass density, specific heat capacity, and volume, respectively, of particle i. Then, it is possible to show that τ_p for particle i,

$$\tau_{pi} = \frac{\rho_i C_{pi} V_i}{H_c}. \tag{2}$$

The contact forces and heat transfer of particle-wall contacts follow the same rules as the particle-particle contacts. The drum wall has a fixed temperature T_w and a periodic boundary along the axial direction [Figs. 1(a), 1(b), and 1(c)]. The particles have initial temperature of T_o. The particle size distribution (based on the number of particles) follows a Gaussian probability distribution. The particle and drum properties, fraction of drum volume filled with particles (fill level) F_L, and ω are varied resulting in a Froude number $(= \frac{\omega^2 D}{2g}$, where D is the drum diameter and g is the gravitational acceleration) between 8.0×10^{-4} and 3.0×10^{-1} (the details of the material properties can be found in the Supplemental Material [20]). The simulations are run until the average temperature of the particles is very close to the wall temperature. The thermal time constant τ is determined based on the evolution of the average temperature from the simulations [Fig. 1(d)].

III. SCALING LAWS

Figure 2(a) shows the relationship between the dimensionless timescales $\frac{\tau}{\tau_c}$ and ϕ for different values of D and ω for a given F_L. For all drum sizes, the relationship between $\frac{\tau}{\tau_c}$ and ϕ follows a power law function $(\frac{\tau}{\tau_c} = a\phi^b)$. The value of the exponent $b \approx 0.88$ is independent of the drum size. Our simulations indicate that this relationship is even valid for $\phi \to 0$ (for a stationary drum $\omega = 0 \Rightarrow \tau_c = \infty$). For a given value of τ_p, τ for stationary drums is greater than that of the rotating drums at $\phi < 1$. Therefore, the drum rotation actually delays the heating process for $\phi < 1$, while drum rotation facilitates the heating process for $\phi > 1$. In other words, for $\phi < 1$, the heat transfer is dominated by granular conduction, while for $\phi > 1$, the heat transfer is dominated by granular convection [15]. The proportionality constant a increases with

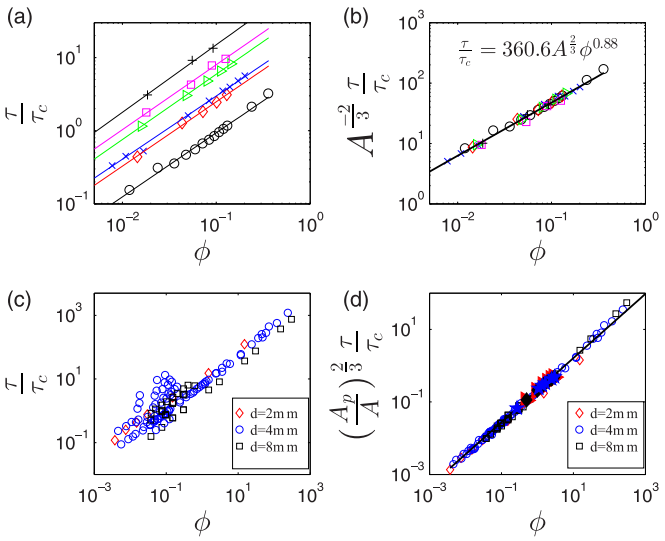

FIG. 2. (a) $\frac{\tau}{\tau_c}$ vs ϕ for various D. For each D, ω is varied between 0.1 and 60 rpm and $\frac{\tau}{\tau_c} = a\phi^{0.88}$. $a = 7.2$ for $D = 15$ (○), $a = 19.2$ for $D = 30$ (◇), $a = 22.4$ for $D = 40$ (×), $a = 47.1$ for $D = 60$ (▷), $a = 62.6$ for $D = 90$ (□), and $a = 125.8$ for $D = 120$ cm (+). ($F_L = 15\%$, $k = 3000$ W/mK, $C_p = 880$ J/kgK, and $\bar{d} = 4$ mm). (b) Same data as in (a) but $\frac{\tau}{\tau_c}$ is normalized by $A^{\frac{2}{3}}$ and the data collapses into a single equation. (c) $\frac{\tau}{\tau_c}$ vs ϕ plot for several values of D and properties listed in the Supplemental Material [20]. The values of ϕ range over four orders of magnitude. (d) Same data as in (c) but normalized by $(\frac{A}{A_p})^{\frac{2}{3}}$ and experimental data for expanded clay (▶), glass beads (◆), and steel balls (★) [7]. The line represents Eq. (3).

the drum size (or equivalently with the amount of granular material, as the amount of material is proportional to D^2 for a constant F_L). This indicates that the time required to heat the particles increases with the amount of material in the drum. It is found that a scales with the fill area $\{A = \frac{D^2}{8}[\theta - \sin(\theta)]\}$, such that $a \sim A^{\frac{2}{3}}$. The data in Fig. 2(a) collapses into a single equation when $\frac{\tau}{\tau_c}$ is normalized by $A^{\frac{2}{3}}$ [Fig. 2(b)]. Using this equation it is possible to predict the average temperature of particles at anytime for any size of drum (for any values of T_w and T_o).

In addition to D and ω, F_L and the mechanical, thermal, and physical properties of the particles also affect τ [Fig. 2(c)]. In general, τ increases as d, ρ, D, F_L, E, and ω increase, but decreases as thermal diffusivity $\frac{k}{C_p}$ increases. However, if D, F_L, and d are kept constant, the relationship between $\frac{\tau}{\tau_c}$ and ϕ remains the same.

Based on the DEM simulation results, we notice that τ depends only on ϕ and a dimensionless area parameter $\frac{A}{A_p}$, which is proportional to the number of particles in the system, where A_p is the projected area of the average particle ($\frac{\pi d^2}{4}$), such that

$$\frac{\tau}{\tau_c} = 0.21\left(\frac{A}{A_p}\right)^{2/3}\phi^{0.88}. \quad (3)$$

Figure 2(d) shows that all simulation data collapse into this single equation [Eq. (3)]. This relationship can be used to predict the average temperature of the particles at any time, for all types of materials, speed of rotation, and fill level. The most significant advantage of Eq. (3) is that it doesn't require any simulation; all the parameters can be determined *a priori*. For practical applications of scale up from laboratory scale experiments to large commercial productions, Eq. (3) has great implications. First, if the material properties of the particles are known, the average temperature of the particles can be predicted without any experiment. Second, if the properties of the particles are not known, an experiment in a small rotating drum can be conducted to determine τ_p, and then the temperature of the particles in a large drum can be predicted based on τ_p (which was computed from the small drum experiment). We used this procedure to determine τ_p for the experiments reported in Nafsun *et al.* [7] for one experiment, and compared our model to the remaining ones of their experimental data [Fig. 2(d)].

IV. TEMPERATURE DISTRIBUTION

The average temperature alone, however, cannot describe the entire heat transfer process, since all particles do not necessarily have the same temperature. To characterize the thermal properties of the entire granular system, it is important to quantify the distribution of individual particle temperature (Fig. 3). Unlike $\bar{T}$, which increases steadily with time, the temperature of individual particles exhibits some fluctuations. It is noted that a particle's temperature rises significantly when the particle is in contact with the wall, but the heat conducts away once the particle is mixed with the bulk. The magnitude of the fluctuation decreases steadily as $\bar{T}$ approaches T_w [Figs. 3(a) and 3(b)].

Figure 3(c) shows the probability distribution function $f(T)$ of individual particles' temperature at $\bar{T} = \frac{T_w+T_o}{2}$ for different values of ϕ. The width of the distribution decreases as ϕ increases. The characteristics (mostly the width) of $f(T)$ evolve with time, but for most instances $f(T)$ may be described

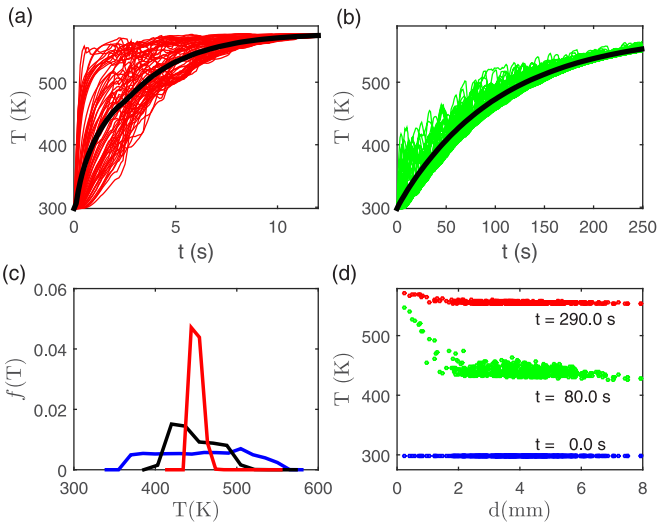

FIG. 3. Evolution of temperature of individual particles for (a) $\phi = 0.03$ (low ϕ case) and (b) $\phi = 35$ (high ϕ case). (c) Probability distribution function of the particles' temperature, $f(T)$, for $\phi = 0.03$ (blue), 3.5 (black), and 35 (red) when $\bar{T} = \frac{T_w+T_o}{2}$. (d) Temperature of individual particles vs size of particles for $\phi = 35$ at $t = 0$ ($\bar{T} = T_o$), $t = 80.0$, and $t = 290.0$ s.

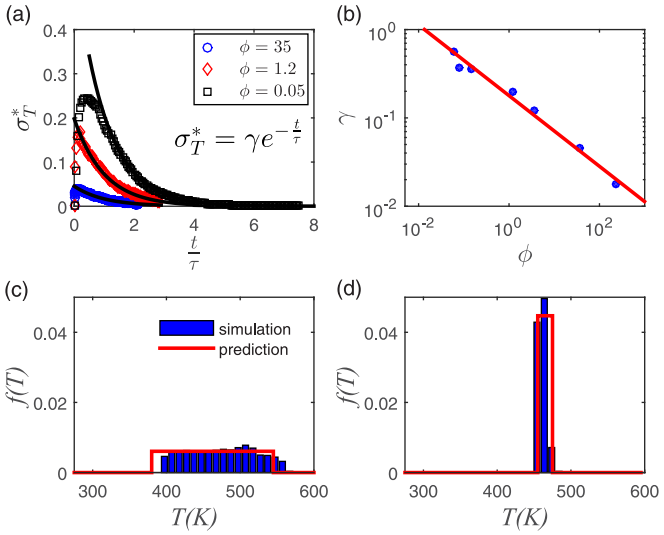

FIG. 4. (a) Evolution of σ_T^* for ϕ =0.05, 1.2, and 35.0 as a function of normalized time $\frac{t}{\tau}$. (b) γ vs ϕ for various values of ϕ; $\gamma \sim \phi^{-2/5}$. (c) $f(T)$ for $\phi = 0.05$ and $\tau = 2.0$ s. (d) $f(T)$ for $\phi = 35$ and $\tau = 115$ s.

by what is commonly known as a uniform (or rectangular) distribution,

$$f(T) = \begin{cases} \frac{1}{T_{\max} - T_{\min}} & \text{if } T_{\min} < T < T_{\max} \\ 0 & \text{otherwise,} \end{cases} \quad (4)$$

where $T_{\min}$ and $T_{\max}$ are the minimum and maximum particle temperatures, respectively. While $T_{\min}$ has a clear profile, $T_{\max}$ can be affected by the particle size distribution. It is noted that the smallest particles percolate to the bottom of the granular material and remain in contact with the wall for the majority of the time. This particle size driven segregation and shorter amount of time required to heat up smaller particles results in higher temperatures for the fine particles than the rest of the particles. This phenomenon is particularly noticeable for high ϕ cases, where $f(T)$ has a narrow width [Figs. 3(c) and 3(d)]. These faster increases in temperature for the fine particles is not observed for a narrow particle size distribution (see Supplemental Material [20]).

If $f(T)$ is assumed to be a uniform distribution, only the average $\bar{T}$ and standard deviation σ_T of the particle temperature are required to predict $f(T)$ at any time during the simulation. The average temperature can be computed based on Eq. (3) for all values of ϕ and the characteristics of σ_T can be studied based on the simulation results. Figure 4(a) shows the evolution of σ_T for some representative values of ϕ. Obviously $\sigma_T = 0$ at the start of the process (because all particles have the same initial temperature T_o) and at the end of the process (because all particles approach the wall temperature T_w). For the entire process σ_T has two important phases. The first phase is a rapid (approximately logarithmic) increase of σ_T during the early stages of the process. The second phase is a relatively slow exponential decay after it has reached a peak at the end of the first phase. Since the exponential decay (second phase) dominates the process (more than 90% of the duration of the simulation) and controls the approach of particles to the target temperature, our focus will be on this phase. The peak of σ_T decreases as ϕ increases, while the exponential decay has a decay rate of $\frac{1}{\tau}$ (similar to the analytic solution of $\bar{T}$), such that

$$\sigma_T^*(t) = \gamma(\phi) e^{-\frac{t}{\tau}}, \quad (5)$$

where $\sigma_T^* = \frac{\sigma_T}{T_w - T_o}$ and γ is a proportionality constant that is a function of only ϕ. Based on our simulations $\gamma(\phi) \approx a_\gamma \phi^{\frac{-2}{5}}$ [Fig. 4(d)]. For our simulations $a_\gamma \approx 0.18$.

Since $\bar{T}$ and σ_T can be predicted from Eqs. (3) and (5), respectively, the two parameters for the uniform distribution [Eq. (4)], $T_{\max}$ and $T_{\min}$, can be determined directly for the entire simulation. $T_{\max} = \bar{T} + \sqrt{3}\sigma_T$ and $T_{\min} = \bar{T} - \sqrt{3}\sigma_T$. $T_{\max}$ and $T_{\min}$ are the only parameters required for describing a uniform distribution. The predictions of $f(T)$ made using these equations are in good agreement with the observations in the simulations [Figs. 4(c) and 4(d)].

V. CONCLUSION

In this article, we have presented a scaling of heat transfer of granular flows in rotating drums that can be used to predict the average temperature and distribution of particles' temperature under a variety of conditions. Our analysis includes the heat transfer contributions from granular conduction and granular convection (mixing), and we have introduced dimensionless equations that can be used for scaling of the heat transfer. The model compares well with experimental results reported in the literature. Compared to other models [4,5], our model has an advantage since we use only particle properties and basic physics principles rather than bulk properties, which can be variable depending on the surrounding conditions. We have included detailed comparisons with some of the prior models in the Supplemental Material [20]. We believe this sets a basis for future studies of heat transfer in granular media that will possibly include heat transfer through a thin gas film between solid contacts, radiation, fluid convection, and granular flows in other types of geometries.

ACKNOWLEDGMENT

We gratefully acknowledge the support of the Rutgers Catalyst Manufacturing Consortium.

[1] A. Watkinson and J. Brimacombe, Metall. Trans. B **13**, 369 (1982); C. Argento and D. Bouvard, Int. J. Heat Mass Transfer **39**, 1343 (1996); S. Felder-Casagrande, H. G. Wiedemann, and A. Reller, J. Therm. Anal. Calorim. **49**, 971 (1997).

[2] J. Lehmberg, M. Hehl, and K. Schügerl, Powder Technol. **18**, 149 (1977).

[3] H. N. Emady, K. V. Anderson, W. G. Borghard, F. J. Muzzio, B. J. Glasser, and A. M. Cuitino, Chem. Eng. Sci. **152**, 45 (2016).

[4] G. Wes, A. Drinkenburg, and S. Stemerding, Powder Technol. **13**, 177 (1976); **13**, 185 (1976).
[5] S. H. Tscheng and A. P. Watkinson, Can. J. Chem. Eng. **57**, 433 (1979).
[6] P. Thammavong, M. Debacq, S. Vitu, and M. Dupoizat, Chem. Eng. Technol. **34**, 707 (2011); A. Boateng and P. Barr, Int. J. Heat Mass Transfer **39**, 2131 (1996).
[7] A. I. Nafsun, F. Herz, E. Specht, V. Scherer, and S. Wirtz, Exp. Heat Transfer **29**, 520 (2016).
[8] F. Herz, I. Mitov, E. Specht, and R. Stanev, Int. J. Heat Mass Transfer **55**, 7941 (2012).
[9] F. Herz, I. Mitov, E. Specht, and R. Stanev, Chem. Eng. Sci. **82**, 312 (2012).
[10] S. Yagi and D. Kunii, AIChE J. **3**, 373 (1957); Y. Ding, R. Forster, J. Seville, and D. Parker, Powder Technol. **121**, 168 (2001).
[11] W. L. Vargas and J. J. McCarthy, AIChE J. **47**, 1052 (2001); I. Figueroa, W. L. Vargas, and J. J. McCarthy, Chem. Eng. Sci. **65**, 1045 (2010); D. Shi, W. L. Vargas, and J. McCarthy, *ibid.* **63**, 4506 (2008).
[12] O. S. Sudah, A. Chester, J. Kowalski, J. Beeckman, and F. Muzzio, Powder Technol. **126**, 166 (2002); B. Chaudhuri, F. J. Muzzio, and M. S. Tomassone, *ibid.* **198**, 6 (2010).
[13] H. Henein, J. Brimacombe, and A. Watkinson, Metall. Trans. B **14**, 191 (1983); M. Kwapinska, G. Saage, and E. Tsotsas, Powder Technol. **161**, 69 (2006).
[14] S.-Q. Li, L.-B. Ma, W. Wan, and Q. Yao, Chem. Eng. Technol. **28**, 1480 (2005); G. Cheng, A. Yu, and P. Zulli, Chem. Eng. Sci. **54**, 4199 (1999); A. Morris, S. Pannala, Z. Ma, and C. Hrenya, Int. J. Heat Mass Transfer **89**, 1277 (2015).
[15] P. Rognon and I. Einav, Phys. Rev. Lett. **105**, 218301 (2010).
[16] G. MiDi, Eur. Phys. J. E **14**, 341 (2004).
[17] H. Hertz, J. Reine Angew. Math. **92**, 156 (1882); R. D. Mindlin and H. Deresiewicz, J. Appl. Mech. **20**, 327 (1953); K. L. Johnson, *Contact mechanics* (Cambridge University Press, Cambridge, 1985); Y. Tsuji, T. Tanaka, and T. Ishida, Powder Tech. **71**, 239 (1992).
[18] G. K. Batchelor and R. W. O'Brien, Proc. R. Soc. London A **355**, 313 (1977).
[19] W. L. Vargas and J. J. McCarthy, Phys. Rev. E **76**, 041301 (2007).
[20] See Supplemental Material at http://link.aps.org/supplemental/10.1103/PhysRevE.94.042902 for additional simulation results, comparison with experiments, and a movie for one of our simulations.